Physics – Uspekhi **66** (6) 628 – 642 (2023)

INSTRUMENTS AND METHODS OF INVESTIGATION PACS numbers: **02.50. – r**, **02.60. – x**, 96.50.S –, 96.50.sb

Review of unfolding methods

Yu V Bogomolov, V V Alekseev, O A Levanova, A G Mayorov, V V Malakhov

DOI: https://doi.org/10.3367/UFNe.2022.05.039189

Contents

Abstract. Very high accuracy and sensitivity have become attainable by modern instruments for experimental measurements of physical quantities in various scientific fields. Yet it is still impossible to completely eliminate the influence of instrumental effects on the result. The measured values of a physical quantity inevitably differ, sometimes significantly, from the true ones. The question therefore arises of restoring the true distributions from the measured ones, taking the specific features of the experiment and the characteristics of scientific instruments into account. Different approaches are in use based on a mathematical model of the instrument and the formulation of the deconvolution problem. We describe this problem, key ideas and methods for its solution, and features and implementation details using the example of elementary particle physics and space physics experiments.

Keywords: unfolding, deconvolution, spectrum restoration methods, statistical estimates, Bayesian methods, regularization, binning-free methods, machine learning

1. Introduction

The precision of modern experiments in various scientific fields is constantly increasing, the tools of science have become more sensitive and the results obtained are more accurate. This allows new discoveries to be made, previously inaccessible effects and phenomena to be explored, and our understanding of the laws of nature to be improved. At the same time, quality requirements for the processing and analysis of the obtained data have to increase in order to eliminate the influence of instrumental effects on the result. The fields of nuclear physics, elementary particles, space physics, and other related disciplines are no exception in this regard.

In this paper, we consider an important issue associated with the processing of scientific data of modern experiments in these fields: given the measured values, to reconstruct the true values of particle characteristics and their distributions.

The inaccuracies of the measuring instruments and equipment noise lead to various distortions in the characteristics of the particles such as speed, magnetic rigidity, energy, momentum, and the direction of motion. As a result, the distributions of these characteristics obtained in experiment, for example, energy spectra and angular and mass distributions, differ from the true ones, which can lead to incorrect interpretations of the measurement results and erroneous physical conclusions.

Such a problem can be solved using so-called deconvolution methods, which allow reconstructing the true distribution of a given characteristic from the measured data; more precisely, an estimate as close as possible to the true but generally unknown law is to be found. These methods use information about the expected nature of the distortions occurring in measurements, obtained by modeling the response of the instrument by Monte Carlo methods or as a result of gauging. Such data with the known true and measured values of a physical quantity are then used to construct a migration matrix [1, 2]. The convolution of the migration matrix with the true distribution gives the measured distribution of this quantity. In processing experimental data, the solution to the inverse problem is of interest, but the convolution of the inverse migration matrix with the measured distribution is an unstable estimate of the true distribution [3–6]. This is why deconvolution algorithms

Yu.V. Bogomolov [1, 2, a], **V.V. Alekseev** [1, 2], **O.A. Levanova** [1, 2, b], **A.G. Mayorov** [2], **V.V. Malakhov** [2]
[1] Demidov Yaroslavl State University, ul. Sovetskaya 14, 150003 Yaroslavl, Russian Federation
[2] National Research Nuclear University MEPhI (Moscow Engineering Physics Institute), Kashirskoe shosse 31, 115409 Moscow, Russian Federation
E-mail: [a] mathematics@inbox.ru, [b] olaydy@gmail.com

Received 23 January 2022, revised 7 April 2022
Uspekhi Fizicheskikh Nauk **193** (6) 669 – 685 (2023)
Translated by S Alekseev

based on various mathematical approaches are used to obtain a stable solution.

Various statistical methods are employed in particle physics [5, 7]. The approaches to solving the deconvolution problem, specific algorithm features, and applications to the processing of experimental results in high-energy physics have been actively discussed since the early 1980s. In 1984, a general review of algorithms for solving this problem was given by Blobel in the framework of the CERN Summer School of Computing and was presented in [1]. In 1998, a detailed description of some of the deconvolution methods was given in a chapter of Cowan's book [8] devoted to statistical data analysis, and also in his review article [5]. The deconvolution methods relevant at the time were described in a subsequent review article by Blobel [9] (2011) and in the chapter he wrote for a practical guide on the use of statistical methods in high-energy physics [10].

These review publications describe the general idea of the problem setup for reconstructing the spectrum of physical quantities and of possible errors when using the 'naive' approach to solving the problem and also provide a detailed (idea-to-algorithm) description of some methods for solving the deconvolution problem. These publications are not without some drawbacks, including a significant bias toward the description of regularization methods for reconstructing the discrete spectrum, resulting in insufficient coverage of other deconvolution methods. We also note that there are no descriptions of the practical use of the corresponding algorithms in these publications. A more extensive review of deconvolution methods was presented in [11–15]. Also of great practical importance are studies [16, 17], which, in addition to reviewing the methods, provide a comparative analysis of the algorithms implemented in the deconvolution software packages that are actively used in processing the results of physical experiments.

Descriptions of deconvolution algorithms can generally be found in a review section or when listing data processing methods in published theses. In some of them, the authors limit themselves to mentioning a particular method they select [18, 19] but occasionally also include a comparative analysis of deconvolution algorithms [20], including a rather detailed review [21].

Deconvolution methods currently continue to be developed: the existing ones are modified and new algorithms are proposed. In particular, machine learning methods, which have proven themselves in various applied fields, are actively used. Such approaches are particularly applicable to constructing estimates of the continuous spectrum using so-called binning-free deconvolution methods, whose prospects of use in applied problems have been actively discussed in the last decade [22–25].

In this paper, we give a broad overview of deconvolution methods for reconstructing discrete and continuous spectra: the basic and most frequently used deconvolution methods are considered in detail, their advantages and disadvantages are discussed, and some general problems important in processing the experimental results are addressed.

2. Deconvolution problem

In this section, we discuss a general approach to reconstructing an estimate of the true distribution of a physical quantity, introduce basic terms and notation, and describe the fundamental problem statement and a direct method for solving it.

2.1 Background

The difference between measured and true values of a physical quantity can be small or large, in the general case leading to a difference between experimental distributions and true ones. There are several reasons why values are measured inaccurately and differ from the true values. Most often, this occurs due to a finite resolving power of the measuring equipment or due to noise, and can also be the result of various physical processes associated with the passage of particles through the substance of the instrument, such as scattering or energy loss.

There is therefore a need to reconstruct the true distribution of a quantity given the measured distribution; this problem can be formulated in the framework of the so-called deconvolution approach, also known as *unfolding* in the literature.

In some cases, the problem setup can be simplified, for example, if the general form of the sought distribution is known and one or several parameters involved in it can be estimated. But, in the general case, the distribution law is unknown, except perhaps for its distinct properties such as continuity or smoothness. This requires the use of nonparametric methods of mathematical statistics. In particular, histogram methods, which resort to dividing a set of values of a given quantity into intervals, density approximation methods based on a system of basis functions, and methods of local density estimates from a sample are used to estimate the distribution density.

The distribution law for values of a physical quantity to be reconstructed can be continuous or discrete. The first option is frequently encountered in scientific problems, and the histogram method with discretization of the continuous spectrum of a physical quantity is then most widely used. In this case, the following approach is used to evaluate the true distribution law of the measured quantity:

- the set of values of the measured quantity is divided into intervals (bins);
- the number of events included in each bin is counted;
- an instrumental histogram is built, which is a discrete approximation of the continuous distribution of the measured value;
- the response function of the instrument is found, taking the difference between the measured and true values into account (migration matrix);
- a statistical estimate of the true distribution is constructed.

We note that the result of reconstructing the true distribution in this case is not a continuous function but a discrete statistical estimate, which in any case differs from the discretization of the true unknown distribution of the relevant physical quantity. However, the use of the deconvolution approach allows obtaining a more accurate statistical estimate that is close to the true law.

Other approaches to solving the problem of reconstructing the distribution laws of a physical quantity, not relying on a system of bins, can be conventionally classified as binning-free methods. In this case, the spectrum reconstruction algorithm is based on a particular idea for estimating the unknown distribution density. The following main approaches can be selected:

- kernel smoothing [26]: an estimate of the unknown continuous distribution density is constructed as the arithmetic mean of the values of a function of a special form (kernel function) at the sampling points;

• projection method [27]: the continuous distribution density is estimated as a linear combination of some system (basis) of functions;

• spline approach [28]: the distribution density is estimated as a piecewise-defined function whose components in each interval are estimated from a sample;

• local method: the distribution density is estimated only in the vicinity of a specific selected point (the method of k-nearest neighbors [29], the method of potential functions [30], and other approaches are used).

We also note that some methods are used in both cases, for constructing discrete estimates (histograms) of the density in a selected system of intervals and for a smoothed estimate of the distribution density. They are described, for example, in [24] and the references therein.

2.2 Notation and problem statement in the case of discretization

We consider a physical quantity whose values are distributed in accordance with an unknown law. As noted in Section 2.1, the most common strategy to estimate the distribution law is to construct estimates of the probabilities that the values of a random variable fall into a certain finite set of intervals. In this case, the range of possible true values can be partitioned into a set of bins $\Delta = (\Delta_1, \Delta_2, \ldots, \Delta_n)$, each of which is associated with the probability of finding the true value inside it. This partitioning procedure is called binning, and the resulting set of probabilities $p = (p_1, p_2, \ldots, p_n)$ is called the discretization of the continuous distribution, or of the true spectrum, whose estimate is to be found.

Partitioning can be arbitrary and nonuniform in general, but the reconstruction quality of the true distribution significantly depends on the choice of binning (this problem is discussed in more detail below).

Let N particles be registered in the experiment, for each of which the value of a chosen quantity is measured; such a single fact is called an event. The expectation value of the true number of events in the bins, denoted by $\tau = (\tau_1, \tau_2, \ldots, \tau_n)$, is calculated as $\tau = Np$.

The range of measured values is also binned, $\Delta' = (\Delta'_1, \Delta'_2, \ldots, \Delta'_k)$. We note that it is acceptable to use different binnings for true and measured values, possibly with $n \neq k$. The number of detected particles in the corresponding bins is denoted by $m = (m_1, m_2, \ldots, m_k)$ and is called the measured spectrum. In some cases, the term is also used for the corresponding frequencies $m/N = (m_1/N, m_2/N, \ldots, m_k/N)$.

In Fig. 1, we illustrate the true and measured spectra of some quantity. The difference between them, due to the above reasons, can be significant for some bins or a sequence of bins.

The difference between the spectra can be described using the migration matrix R whose R_{ij} entry is the probability that the true value of the quantity from the jth bin is registered in the ith bin. Then, the expectation values $\nu = (\nu_1, \nu_2, \ldots, \nu_k)$ of the number of events with characteristic values lying in the considered bins are given by $\nu = R\tau$.

In Fig. 2, we show an example of the migration matrix with different partitions into bins along the axes of the true and measured values of a physical quantity; color coding shows the values of the migration matrix entries R_{ij}.

The main task is therefore to develop methods for a consistent statistical evaluation of the unknowns p or the expectation values τ proportional to them, given the measured spectrum m with a known nature of distortions described with a migration matrix R.

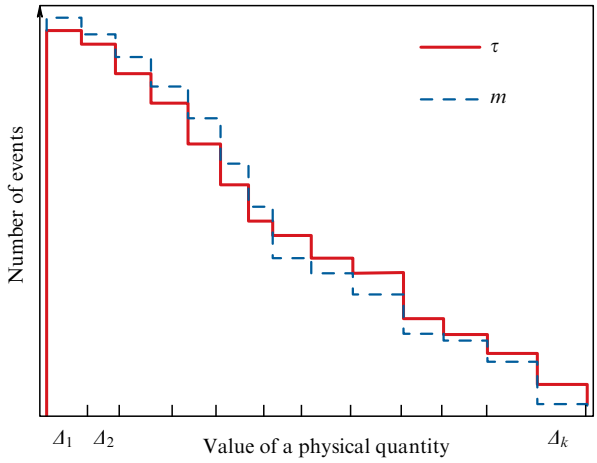

Figure 1. Illustration of the true (solid line) and measured (dashed line) distributions of a physical quantity.

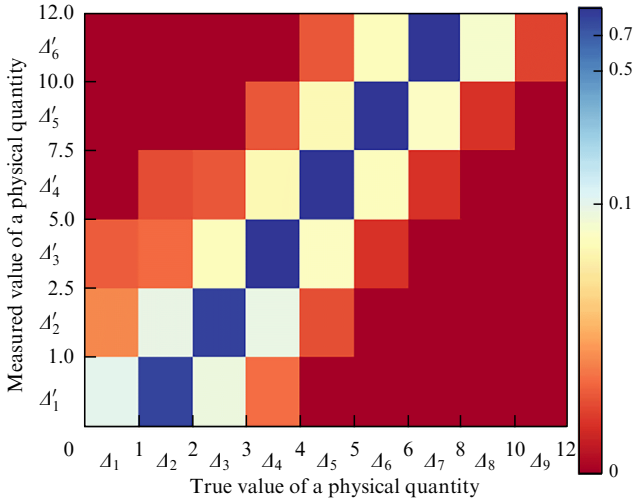

Figure 2. Illustrative representation of the migration matrix.

2.3 Direct method for solving the deconvolution problem

To solve the problem, it is natural to assume that events cannot occur simultaneously (the ordinariness condition). The probability of registering a fixed number of events m_i in the interval Δ_i during the observation time must be independent of the occurrence of events at preceding instants (no aftereffect) and of the chosen zero of observation time (stationarity condition). Under these assumptions, all the necessary conditions are satisfied that allow considering the sequence of events to be the simplest, Poisson, flow [2].

The number of events that fall into the interval Δ_i is then a Poisson-distributed random variable with the expectation value ν_i. The probability of the occurrence of m_i such events is

$$P(m_i, \nu_i) = \exp(-\nu_i)\,\frac{\nu_i^{m_i}}{m_i!}\,.$$

We thus consider a set of Poisson-distributed random variables with unknown expectation values ν, which in turn depend on the unknown τ ($\nu = R\tau$). To construct a consistent statistical estimate of τ for a sample m, the maximum likelihood method can be used. For this, the

likelihood function is constructed and maximized with respect to τ:

$$L(\tau) = \prod_i P(m_i, \nu_i) = \prod_i \exp(-\nu_i) \frac{\nu_i^{m_i}}{m_i!} \to \max_\tau .$$

The constructed likelihood function $L(\tau)$ reaches a maximum at $\nu_i = m_i$, and τ can be estimated as $\hat{\tau} = R^{-1}m$ [3, 5]. This corresponds to the 'naive' approach to solving the deconvolution problem: the measured and true distributions are assumed to be related by a linear matrix equation, which is solved by applying the inverse migration matrix to the measured spectrum.

The constructed point estimate $\hat{\tau}$ is consistent and unbiased [5, 31–33]. In practice, however, the use of the direct method is only possible for a large sample size and a very high resolution of the measuring instruments, which corresponds to a nearly diagonal matrix R [3, 5]. Otherwise, the estimate is sensitive to small perturbations of the measured distribution (i.e., the direct estimate is unstable), which leads to an unacceptably large error (uncertainty) in the estimate of τ [3–6]. At the same time, it is impossible to exactly draw the applicability bound of the direct method that would ensure its stability, because in general it depends on a large number of factors unique to each experiment, and each case requires a separate study.

In addition to the noted instability, the described approach in its original form does not allow taking the features of the true distribution into account, such as its smoothness or entropy [8, 34].

The combination of these shortcomings does not allow the direct method to be widely used to estimate the true distribution, because it does not guarantee a well-defined stable result. A possible solution is to artificially introduce a bias into the statistical estimate, which can be done following the two most common strategies [35]:

(1) adding a 'penalty' term to the likelihood function (on which the methods using Tikhonov's regularization are based, to be discussed below) [36, 37];

(2) early stopping of iterative algorithms for constructing statistical estimates [38].

In Section 3, special methods for solving this problem are discussed in detail, based on various mathematical algorithms for deconvolution and the ideas involving biased estimates.

3. Methods for solving the deconvolution problem

To reduce statistical errors and smooth the estimate of the true distribution, certain modifications of the direct method as well as fundamentally different approaches to deconvolution are used, including the following ones:

(1) Bayesian approaches to solving the inverse convolution problem [39] (D'Agostini methods [38, 40], modifications of Kuusela, Panaretos [41, 42]), the FBU (fully Bayesian unfolding) algorithm [43];

(2) Tikhonov's regularization and its modifications (singular value decomposition, SVD: Kartvelishvili, Höcker [36, 44], entropy-based regularization [5], and the TUnfold method implemented in the ROOT software package [12, 37]);

(3) introduction of correction factors and systematic shifts (model dependence) [5];

(4) machine learning methods.

3.1 Bayesian methods

A common approach to solving the deconvolution problem is the idea of using the Bayes formula to estimate the probabilities of particles falling into bins according to the frequencies of observed events and the available migration matrix. We describe how this approach can be applied to the problem of reconstructing the spectrum of a physical quantity.

We let $C_1, C_2, \ldots, C_n$ denote events associated with the actual occurrence of a physical quantity in the corresponding bin $\Delta_1, \Delta_2, \ldots, \Delta_n$. Events associated with event detection in the same bins are denoted by $E_1, E_2, \ldots, E_n$. We note that the probabilities $P(C_1), P(C_2), \ldots, P(C_n)$ are unknown: they are the components of the sought true spectrum ($p_i = P(C_i)$), and the probabilities of the particles being detected in the bins can be estimated from the experimental results as $\hat{P}(E_j) = m_j/N$. Also, using gauging data or numerical simulation, we can estimate the conditional probabilities of detecting a characteristic in a jth bin if the value actually falls into an ith bin. In the foregoing, these conditional probabilities were interpreted as entries of the migration matrix $R_{ij} = P(E_j|C_i)$.

The deconvolution procedure is thus reformulated in terms of events and their probabilities as a problem of reconstructing unknown probabilities $P(C_i)$ or expectation values proportional to them for the true number of events in the corresponding bins given the conditional probabilities $P(E_j|C_i)$ and the probabilities $P(E_j)$ (experimentally estimated as $\hat{P}(E_j)$). To solve this problem, we must estimate the conditional probability of actually finding a physical quantity in the jth bin if it is detected in the ith bin. This is done in accordance with the Bayes formula

$$M_{ji} = P(C_i|E_j) = \frac{P(E_j|C_i)P(C_i)}{P(E_j)} = \frac{P(E_j|C_i)P(C_i)}{\sum_{k=1}^n P(C_k)P(E_j|C_k)} .$$

Then, the expectation value of the number of events detected in the jth bin (the total number of such events being m_j) if the true value lies in the ith bin is estimated as $m_j P(C_i|E_j) = M_{ji}m_j$. Accordingly, the expectation value of the true number of events in the ith bin is obtained by summing over all bins in which events are detected: $\hat{\tau}_i = \sum_{j=1}^n M_{ji}\, m_j$. The resultant matrix $M = (M_{ji})$ is called the deconvolution matrix; in general, it is not the inverse of the migration matrix R.

In practice, it should be taken into account that a physical quantity from the jth bin can be detected outside the considered range. The probability of registration in at least one of the considered bins is called the efficiency and is defined as $\varepsilon_j = \sum_{k=1}^n P(E_j|C_k)$. If $\varepsilon_j \neq 1$, the expected true number of events in the jth bin is calculated as $\hat{\tau}_i = (1/\varepsilon_i) \sum_{j=1}^n M_{ji}\, m_j$. We assume in what follows that the correction for the efficiency is absorbed into the matrix M, and also call the resultant matrix the deconvolution matrix.

The deconvolution problem (estimating the true spectrum) reduces to constructing the matrix M. However, the Bayes formula for estimating the entries M_{ji} involves the probabilities $P(C_i)$ that are the unknowns. In other words, to estimate the true spectrum with this approach, the probability distribution of the occurrence of a physical quantity over the corresponding bins (i.e., the true spectrum itself) should already be known, which makes the deconvolution problem ill posed. It is impossible to estimate the probabilities $P(C_i)$ (unlike $P(E_j)$) directly from experimental data. To reconstruct the true spectrum, the method described by D'Agostini

[38] is therefore used, which is based on the approach known in other fields as the Richardson–Lucy algorithm [45–48]. The method is based on the idea that some initial approximation of the true spectrum can be chosen and then successively refined. To construct the required matrix M, the current estimate of the true spectrum is used as an estimate of the probabilities $P(C_i)$ in the Bayes formula. Assuming that such a procedure for successively improving the estimate converges, the limit distribution is taken as the solution to the deconvolution problem.

In the ROOT [49] and RooUnfold [50] packages, this idea is implemented as an iterative algorithm as follows.

(1) As the initial approximation of the unknown probabilities $P(C_i)$, take an arbitrary probability distribution $P_0(C_i)$. It is better to choose a distribution that is close to the true one (such an a priori distribution is typically selected based on known physical concepts). When that is impossible, the discrete uniform distribution $P_0(C_j) = 1/k$ can be selected as the first approximation.

(2) Using the Bayes formula, build an estimate of the true distribution

$$M_{ji} = \frac{R_{ij} P_0(C_i)}{\sum_{k=1}^{n} \left(P(E_j|C_k) \sum_{l=1}^{n} R_{kl} P_0(C_l) \right)} ,$$

$$\hat{\tau}_i = \sum_{j=1}^{n} M_{ji} m_j , \qquad \hat{P}(C_i) = \frac{\hat{\tau}_i}{\sum_{k=1}^{n} \hat{\tau}_k} .$$

(3) Estimate the differences between the distribution found in step 2 and the initializing distribution of a true random variable (by the χ^2 or another goodness-of-fit criterion).

(4) Choose the constructed estimate $\hat{P}(C_i)$ as a new initializing distribution $P_0(C_i)$ and repeat steps 2–4 until the discrepancies between the next estimate and the initializing distribution become sufficiently small (less than a critical value).

The most significant drawback of this implementation is the open question about the convergence of the iterative process. We also note that the convergence of an iterative process does not imply the construction of a sufficiently accurate estimate: with a large number of iterations, statistical errors can accumulate, which leads to large deviations of the reconstructed spectrum from the true one [31]. On the contrary, an early stop of the iterative process with small changes in distributions at neighboring iterations, as noted, is considered a possible way to construct biased estimates, albeit with a lower variance [31, 32, 38]. Therefore, the number of iterations required for an acceptable solution to the spectrum reconstruction problem has to be found in the course of a series of numerical experiments with model distributions.

For example, the version of the algorithm implemented in the RooUnfold package uses the following basic idea of stopping the iterative process. At the end of each iteration, two distributions of the random variable of interest are considered: the current distribution and a new distribution built from it as indicated above. The hypothesis about the homogeneity of the distribution laws is analyzed: if the hypothesis is true, then the step of the iterative process has not made a significant impact on the distribution law of the random variable, and hence further iterations are impractical. Alternatively, the rejected homogeneity hypothesis can be interpreted as a noticeable change in the distribution law (spectrum) at the current step, indicating the divergence of the iterative process. In [38, 40], it is proposed that Pearson's χ^2 criterion (and the corresponding metric for the difference between the current and new distributions) be used to test this hypothesis. The number of iterations required to reach the specified stopping criterion is not known in advance. We note that the implementation in the RooUnfold package allows specifying the number of iterations explicitly, thereby allowing more flexible control over the stopping of the iteration process. In particular, the authors of the package use four iterations to illustrate the operation of the algorithm; similar results were obtained when processing data in ALICE (A Large Ion Collider Experiment) [51] at the Large Hadron Collider (LHC).

The described algorithm is based on the idea of iteratively adjusting the occurrence probabilities for each considered bin separately using the Bayes formula. Later, the author of [40] proposed a modified method based on the key idea to reconstruct the distribution of the number of events in bins under the assumption that the distribution is multinomial. The distribution parameters are also iteratively adjusted based on the Bayesian approach. For the stopping criterion of the iterative process, the same procedure is used as in the original method. An important task is therefore to analyze the conditions under which this stopping criterion leads to a correct reconstruction of the distribution and conditions for the convergence of iterations.

3.2 Regularization-based methods

We describe the approach to solving the deconvolution problem based on regularization.

Let us recall that the direct solution to the deconvolution problem is unstable (sensitive to small perturbations). A regularization consists in imposing additional constraints on the functional of the original optimization problem [52] so as to prevent significantly different solutions from being constructed for small variations in the data.

The proposal is therefore to maximize not the original likelihood function (or its logarithm $\ln L(\tau)$) but a function that includes an additional term or multiplier. The extra term may be characteristic of some features of the original distribution (for example, its smoothness). The problem amounts to finding a distribution such that the optimal value of the likelihood function is not reached, but the resulting estimate is stable with respect to perturbations of the measured distributions.

The deconvolution problem can thus be written as the optimization problem

$$\Phi(\tau) = \ln L(\tau) + \alpha S(\tau) \to \max_{\tau} ,$$

where α is a numerical indicator (regularization parameter) describing the contribution of the function $S(\tau)$ (for example, reflecting the expected features of the reconstructed distribution).

The regularization function $S(\tau)$ should be understood as a penalty for violation of the necessary properties of the solution, which are established on the basis of physical considerations, or empirical or theoretical information about the general properties of the measured quantity. Therefore, $S(\tau)$ is chosen such that its maximum value is achieved for distributions τ that have the specified properties. For example, if the expected continuous distribution is characterized by the absence of large fluctuations when passing to a neighboring bin, then it is natural to choose a

regularization function that takes large values for small deviations of the distribution in neighboring bins. An example of such a function corresponding to the distribution smoothness property is

$$S_1(\tau) = -\sum_{i=1}^{n-1}(\tau_{i+1} - \tau_i)^2$$

(an analogue of the first-order derivative). When using the second-order difference, the regularization term has the form

$$S_2(\tau) = -\sum_{i=2}^{n-1}(\tau_{i+1} - 2\tau_i + \tau_{i-1})^2 ,$$

which corresponds to Tikhonov's regularization. Similarly, we can consider functions that reflect higher orders of smoothness. It is also possible to take the nonuniformity of binning into account, which, on the one hand, complicates the form of the regularization term, but, on the other hand, improves the estimate of distribution fluctuations. Some methods use regularization terms corresponding to the entropy of the sought distribution, for example,

$$S_e(\tau) = -\sum_{i=1}^{n}\tau_i \ln \tau_i .$$

We note that a combination of several regularization terms can be used.

For $\alpha = 0$, the solution to the maximization problem coincides with the previously obtained direct solution to the problem (with all its inherent shortcomings). For large α, a distribution is obtained that has the specified properties, but is practically independent of the sample (model-independent).

Methods based on the idea of regularization differ in the following features.

(1) the choice of the type of likelihood function and regularization function:

• the SVD unfolding method (Kartvelishvili, Höcker [36, 44]): a regularization function reflecting the continuity of the distribution;

• the TUnfold method of the ROOT package (Schmitt [16, 37, 53]): a combination of two regularization functions that reflect the continuity or smoothness of the distribution and also limit the estimate bias;

• entropy-based methods: the MRX (method of reduced cross-entropy) (Schmelling [54]), the image reconstruction method (Narayan, Nityananda [55]), the ARU (Automatic Regularized Unfolding) method (Dembinski, Roth [56]);

(2) the choice of the regularization parameter for which the necessary balance is to be achieved between the bias of the distribution estimate and the spread (statistical error) in constructing a point estimate of the distribution.

3.2.1 SVD unfolding method. This method is based on Tikhonov's regularization and the solution of the corresponding system of equations by the SVD of matrices, which allows finding approximate solutions of flawed (for example, overdetermined) systems of linear equations [36, 44]. The problem reduces to minimizing the following function based on the previously described likelihood function:

$$\Phi(\tau) = (R\tau - m)^{\mathrm{T}}(R\tau - m) + \alpha\sum_{i=2}^{n-1}(\tau_{i-1} - 2\tau_i + \tau_{i+1})^2 .$$

Let us briefly describe this approach. The SVD of a matrix A is its representation in the form

$$A = USV^{\mathrm{T}} ,$$

where a real-valued matrix A has size $l \times k$, U and V are orthogonal matrices of the respective sizes $l \times l$ and $k \times k$, and S is a diagonal $l \times k$ matrix (the diagonal entries s_{ii} are nonnegative and are called singular values, and S is called the singular matrix). By choosing the matrices U and V, the singular values can be arranged in descending order. In the case $k = l$, matrices U, S, and V are square $(k \times k)$.

The system of linear equations $A\tau = m$ is exactly solved using the SVD as follows. We write the system as

$$USV^{\mathrm{T}}\tau = m ,$$

and make the change of variables

$$z = V^{\mathrm{T}}\tau , \qquad d = U^{\mathrm{T}}m .$$

As a result, the system takes the form

$$Sz = d ,$$

with the solution

$$z_i = \frac{d_i}{s_{ii}} .$$

This yields the solution of the original system of equations

$$\tau = Vz .$$

For ill-conditioned matrices A, the following pattern is typical: when the system is solved as described, the d_i and the corresponding s_{ii} are small, and hence their small perturbations lead to significant errors in the solutions z_i and the corresponding solutions of the original system τ.

The direct method for spectrum reconstruction is by explicitly solving the system $R\tau = m$, which is equivalent to solving the minimization problem

$$(R\tau - m)^{\mathrm{T}}(R\tau - m) \to \min_{\tau} .$$

The authors of the SVD-based deconvolution method suggest using an approach based on Tikhonov's regularization to find the true spectrum, which allows posing the corresponding minimization problem

$$\Phi(\tau) = (R\tau - m)^{\mathrm{T}}(R\tau - m) + \alpha(C\tau)^{\mathrm{T}}(C\tau) \to \min_{\tau} ,$$

where α is a regularization coefficient (to be defined below) and the matrix C satisfies the equality

$$(C\tau)^{\mathrm{T}}(C\tau) = \sum_{i=2}^{n-1}(\tau_{i-1} - 2\tau_i + \tau_{i+1})^2 .$$

The solution to the described minimization problem is obtained as a solution of the overdetermined extended system of equations

$$\begin{bmatrix} AC^{-1} \\ \sqrt{\alpha}\, I \end{bmatrix} C\tau = \begin{bmatrix} m \\ 0 \end{bmatrix} .$$

We note that the matrix C is degenerate, and therefore has no inverse. To solve this problem, it is recommended to consider a modified matrix $\tilde{C} = C + \xi I$, where the parameter ξ is chosen such that constructing the inverse matrix is possible.

To reduce errors, the authors of the method [36, 44] also recommend renormalizing [36] the equations of the original linear system $R\tau = m$ (such that each equation makes the same 'contribution') so as to have a unit covariance matrix corresponding to the right-hand side of the original system (the measured values). This is achieved by the following algorithm.

(1) Representing the right-hand side of the original system in matrix form, such that the system is written as $R\tau = B$. For the current implementation, $B = \operatorname{diag} m$, and in general B is the covariance matrix of a vector of measured values.

(2) Using the SVD on the right-hand side of the resulting system,

$$B = Q\Lambda Q^{\mathrm{T}},$$

where $l_i^2 = \Lambda_{ii} > 0$, $\Lambda_{ij} = 0$ for $i \neq j$, and

$$B^{-1} = Q\Lambda^{-1}Q^{\mathrm{T}}.$$

(3) Normalizing the left- and right-hand sides of the equation:

$$\tilde{R}_{ij} = \frac{1}{l_i}\sum_k Q_{ik}R_{kj}, \qquad \tilde{m}_i = \frac{1}{l_i}\sum_k Q_{ik}m_k.$$

The result is a renormalized system of equations $\tilde{R}\tau = \tilde{m}$, to which all the operations described previously (introducing a regularization term and solving the extended system) are applied. The new system is solved in the manner described above, but with the intermediate solutions z_i now given by

$$z_i = \frac{d_i}{s_{ii}}\frac{s_{ii}^2}{s_{ii}^2 + \alpha}.$$

Note that, in the case $s_{ii}^2 \gg \alpha$, the solutions are practically coincident with the considered direct solution to the original problem. For small singular values s_{ii}, the effect of the additional regularization term already becomes more pronounced. To find the 'effective value' of the regularization parameter, it is recommended to visually analyze the singular values on a logarithmic scale: plot $\log s_{ii}$, select its linear section, and choose the value $i = k$ at which the monotonic linear decrease in $\log s_{ii}$ is replaced with a sharp drop. The value $\alpha = s_{ii}^2$ (the 'last large' singular value s_{kk}) is then chosen as the regularization coefficient [36]. We note that this spectrum reconstruction algorithm can also be used at other values of the regularization coefficient.

3.2.2 TUnfold method. The algorithm implemented in the ROOT and RooUnfold packages as the TUnfold procedure [16, 37, 53] is also based on the idea of a regularization. It involves minimizing the likelihood function of the form

$$\Phi(\tau) = L_1(\tau) + \alpha L_2(\tau) + \lambda L_3(\tau).$$

Here, the term $L_1 = (R\tau - m)^{\mathrm{T}}(R\tau - m)$ corresponds to the original likelihood function in the direct spectrum reconstruction method: if the coefficients of the remaining terms are set to zero, the estimate of the true distribution as the minimum point of the likelihood function coincides with that constructed with the direct method, which in practice leads to large errors. The L_2 term ensures the expected characteristics of the original distribution (for example, its continuity or smoothness). As such a term, the functions S_1 or S_2, previously introduced in the general description of regularization-based methods, can be chosen. Finally, the function $L_3(\tau) = \sum_i m_i - e^{\mathrm{T}}\tau$ is used in the last term, where the components of the vector e are $e_j = \sum_i R_{ij}$. This term is needed to limit an excessively large bias in the resulting distribution estimate [37].

In regularization-based methods, an important step in solving the problem is the choice of the coefficients at the regularization terms. For example, in the SVD method described in Section 3.2.1, the regularization coefficient was chosen based on the analysis of singular values, but this is highly dependent on the method for solving the distribution reconstruction problem itself. In the TUnfold algorithm [37], the regularization coefficients are not specified, but are automatically selected by one of two methods:

(1) *The L-curve method.* This method is based on solving the maximization problem $\Phi(\tau) = \ln L(\tau) + \alpha S(\tau) \to \max_\tau$. Such a problem is successively solved for different values of α in a certain range with a certain step. The values of the $L(\tau)$ and $S(\tau)$ terms for which the objective function attains a maximum at the current value of α are denoted as L_α and S_α. We take the logarithms of these values, $\mathcal{L}_x(\alpha) = \log L_\alpha$ and $\mathcal{L}_y(\alpha) = \log S_\alpha$, and then construct a parametric curve given the points $(\mathcal{L}_x(\alpha), \mathcal{L}_y(\alpha))$ (to ensure sufficient smoothness, the constructed curve is approximated by a cubic spline). As the sought value of α in the regularization term, we choose the one for which the curvature of the constructed curve is maximum at the corresponding point [12, 13, 37].

(2) *The method of minimizing correlation coefficients*. The values of τ_i can be considered a set of random variables for which the covariance matrix $V_{\tau\tau}$ is to be estimated. To construct this estimate for a chosen value of the regularization coefficient α, a series of computational experiments to reconstruct the spectrum is carried out; as a result, a sample $(\tau_1^k, \ldots, \tau_n^k)$ is formed, where $k = 1, \ldots, K$. Based on this sample, an estimate of the covariance matrix $V_{\tau\tau}$ is constructed. The values of the global correlation coefficient ρ_i for the ith bin are found for different values of α as

$$\rho_i(\alpha) = \sqrt{1 - \frac{1}{(V_{\tau\tau}^{-1})_{ii}(V_{\tau\tau})_{ii}}}.$$

As the optimal value of the regularization coefficient, we choose α, which ensures the minimum value of the arithmetic mean $\rho_i(\alpha)$ or the maximum value of all the $\rho_i(\alpha)$ [2, 12, 37].

Note that these methods proposed for TUnfold for selecting the regularization parameter are universal and can be used in other algorithms. In the same problem, other approaches are also being used, including the modified maximum likelihood estimator (MMLE) method [41], the generalized (weighted) cross-validation method [57], the Akaike information criterion [58, 59], and stopping according to a goodness-of-fit criterion [60].

The idea of using Tikhonov's regularization for deconvolution has long been employed. In elementary particle physics, its wide use started after the development of a regularization algorithm implemented in the $\mathcal{RUN}$ package [1, 61].

There are other methods for solving the deconvolution problem based on the same idea. In particular, we note approaches where the form of the regularization term is based on the entropy of a random variable distribution (regularization by the maximum entropy method) [55, 62]. In this case, the regularization term can have the form

$$S_{\mathrm{e}}(\tau) = -\sum_{i=1}^{n} \tau_i \log \tau_i \quad \text{or} \quad S_{\mathrm{ent}}(\tau) = -\sum_{i=1}^{n} \frac{\tau_i}{N} \log \frac{\tau_i}{N} .$$

In the second case, the authors of the method propose using $\alpha = 1/N$ as the regularization coefficient, but in practice this leads to an overly smoothed distribution [11] (the entropy maximum corresponds to the uniform discrete distribution), and it is therefore advisable to use smaller values of the regularization coefficient.

In addition, a method based on minimizing the variance of the true distribution and combining regularization terms of different types was proposed in [63]. The choice of a specific regularization method is typically determined by a priori information characterizing the features of the initial distribution and its distortion during the measurement.

The idea of using the SVD approach was also developed in the Wiener–SVD method [64]. In addition to the previously described SVD algorithm, the authors use a Wiener filter to reduce the effect of noise. At the same time, the construction of the Wiener filter requires a fairly good estimate of the true spectrum, which is a complication in using the algorithm.

The regularization-based approach is also used in iterative deconvolution algorithms. In particular, the IDS method (iterative, dynamically stabilized method of data unfolding) [65, 66] involves a dynamically changing regularization term, which allows reducing the fluctuations of the reconstructed spectrum in successive iterations.

3.3 Bin-by-bin correction method

There are other approaches to reconstructing the true spectrum in addition to those described in Sections 3.1 and 3.2. One of the simplest is the so-called bin-by-bin correction method. In its simple implementation, numerical simulation is used to obtain the true and measured (distorted) distributions of the considered physical quantity. For each bin, the correction coefficient C_i is calculated as an estimate of how many times the measured number of particles that fall into the bin differs from the true one. The true spectrum estimate is calculated by dividing the measured spectrum by the correction coefficient in each of the bins, $\hat{\tau}_i = \mu_i / C_i$.

In this form, the approach has a number of disadvantages that limit its use in practice [12, 67, 68]. In order to find the correct values of the correction coefficients, the true distribution of particles over the bins has to be known, but estimating this distribution is the original problem. It is worth noting that the procedure for calculating the correction coefficients differs from finding the migration matrix: in the first case, it is crucial to determine the true distribution or its good estimate, and, in the second, this does not play such an important role: it suffices to estimate the probabilities with which a particle is detected in other bins (moreover, to construct an estimate, it is important to have a sufficiently large number of events, but information about how these events should be distributed over the bins is of no principal importance). Finally, the described simple approach does not take migration between bins (even the neighboring ones) into account, and therefore the implementation does not include a reverse redistribution of events between bins; only a mechanistic adjustment is used (as a result, the total number of events may change).

There are also modifications of the bin-by-bin method that somewhat mitigate these shortcomings. For example, an iterative process can be used to reconstruct the spectrum such that the above procedure for calculating the correction coefficients is only a first step [69, 70]. This approach involves refining the correction coefficients at the next step of the algorithm using the preceding spectrum estimate and adjusting the parameters of the Monte Carlo method, which simulates instrumental spectrum distortions [69].

Nevertheless, the use of the bin-by-bin method (including in the simple form) is acceptable if migration between bins is low (the migration matrix is nearly diagonal) [8, 11, 32]. Under this condition, the method is used in the processing of experimental data in modern particle physics [43, 71, 72].

3.4 Other spectrum reconstruction methods

Other deconvolution methods involve both the already noted approaches (iterative methods for constructing estimates, regularization, bin-by-bin correction of distributions) and other mathematical ideas and principles. In particular, algorithms based on an iterative construction of statistical estimates of the distribution of an unknown quantity have been used for a long time. In the early 1930s, van Cittert proposed an iterative method for reconstructing distorted spectra [73, 74], in which the current spectrum estimate is corrected by an amount depending on how much the distortion of the current estimate deviates from the measurement results:

$$\tau^{(k+1)} = \tau^{(k)} + \alpha\left(m - R\tau^{(k)}\right) .$$

An extension of this approach is manifested in the algorithm proposed by Gold in 1964 [75] and subsequently used in particle physics [18, 21, 76]. A characteristic feature of this method is the use of the coefficients

$$\alpha_i^{(k)} = \frac{\tau_i^{(k)}}{\sum_{j=1}^{n} R_{ij}\tau_j^{(k)}}$$

for different bins [75, 77], with the spectrum estimate constructed at the next iteration as

$$\tau_i^{(k+1)} = \tau_i^{(k)} + \alpha_i\left(m_i - \sum_{j=1}^{n} R_{ij}\tau_j^{(k)}\right) .$$

The iterative procedure of Gold's algorithm can also be written as a successive refinement of the current estimate in the current bin by multiplying by some correction coefficient. A similar approach is used in the previously mentioned Richardson–Lucy algorithm [45, 46], which was originally designed for processing astronomical images [78] and later adapted, among other things, for problems of spectrum reconstruction in particle physics experiments [79, 80].

Some deconvolution algorithms are being developed to solve highly specialized physical problems or to analyze the features of specific measuring instruments. For example, in studying neutron fluxes, deconvolution methods are used that are specific to the problem of reconstructing spectra obtained using Bonner spheres. Among such methods, we mention the SPUNIT [81], BON [82], SAND-II [83, 84], MAXED [85], and GRAVEL [86] algorithms.

The previously described deconvolution methods were used to reconstruct the distributions of a physical quantity based on a preliminary partition of the working range of its values into bins. The estimates obtained were discretized estimates of the true distribution. However, this approach has some drawbacks or features that make it difficult to use in practice [24]. First, the working range has to be partitioned into bins in advance, a procedure that is performed manually in most cases [61, 87–90]. Second, the grouping of data by bins amounts to coarse-graining [61], which precludes the flexibility needed to take all additional factors that affect the instrumental response into account, which leads to nonoptimum spectrum estimates. Finally, histogram methods are difficult to adapt when reconstructing distributions of multivariate random quantities. These features motivate focusing attention on approaches in which the true spectrum is estimated without preliminary binning.

To construct distribution density estimates without discretization, approaches based on machine learning methods [91–94] can be used (which are suitable for estimating discretized distributions as well). The main idea is to use the results of numerical simulation as a training sample for designing a prediction system (for example, the modeled true distribution given a modeled measured one) or a classifier. A neural network [92] or a regression model [93] can be chosen as a tool for solving the deconvolution problem, with the input given by the measured values of the considered quantity or the fully measured spectrum and the output being the true value of the considered quantity or the true bin into which this value falls, or the reconstructed true spectrum.

An approach based on the generative adversarial network (GAN) model [95] is also in use: a generative network iteratively generates samples corresponding to the assumed true distribution of the quantity under consideration, and a discriminative network evaluates their fit with the measured distribution, given the known character of distortions (the procedure is similar to the construction of the migration matrix based on numerical simulation) [91, 96]. Difficulties in applying the described approaches in practice are similar to those associated with the use of the bin-by-bin correction method described above.

Another possible approach to describing the estimated distribution density is its representation as a spline function. This method is implemented, in particular, in the ARU algorithm [23, 56, 97], whose development was largely influenced by the ideas proposed in [1, 54]. Here, the sought continuous distribution density $f(x)$ is represented as a cubic B-spline [98] $f(x) = \sum c_j b_j(x)$ with the unknown (estimated) coefficients c_j and arbitrarily chosen nodes. The intervals between nodes should be narrow enough to properly reflect all the features of the sought distribution density, but their number and location are not critical. The distortion of this distribution density is described by the convolution

$$g(y) = \int K(y,x)\, f(x)\, \mathrm{d}x = \sum_j c_j g_j(y)\,,$$

where the distorted basis functions

$$g_j(y) = \int K(y,x) b_j(x)\, \mathrm{d}x$$

are estimated numerically in the proposed algorithm. The convolution kernel $K(y,x)$ is estimated when calibrating or simulating the instrumental response by Monte Carlo methods, similarly to what is done when constructing the migration matrix in the methods described above. The estimate of the coefficients c_j corresponds to the minimum of the negative likelihood function $L(c) = L_1(c) + \lambda L_2(c)$. The first term has the form

$$L_1(c) = \sum_j c_j G_j - \sum \ln g(y_i)\,,$$

where $G_j = \int g_j(y)\, \mathrm{d}y$ and y_i are the measured values of a physical quantity. The second term is the regularization function taken with a coefficient λ,

$$L_2(c) = \int f(x) \ln \frac{f(x)}{h(x)}\, \mathrm{d}x - \sum_j c_j F_j\,,$$

where the first term is the Kullback–Leibler distance from the sought distribution density f to some estimated density h, and $F_j = \int f_j(x)\, \mathrm{d}x$. A separate section of paper [56] is devoted to the choice of the expected density $h(x)$; the authors recommend taking $h(x)$ to be a function closest to the sought distribution density if such information is available a priori. As a rough approximation for $h(x)$, one can take a uniform distribution over the range of values under consideration or perform the first reconstruction of the spectrum using the uniform distribution $h_0(x)$ (yielding an estimate of the reconstructed spectrum $f_0(x)$), and then take $h(x)$ to be the convolution of $f_0(x)$ with the kernel $K(y,x)$ and, based on the function obtained, perform the final spectrum reconstruction procedure.

Some of the approaches used in histogram deconvolution methods can be adapted for the continuous (binning-free) case. For example, the iterative construction of a discretized spectrum estimate served as the main idea for the development of the OmniFold algorithm [24].

As we have noted, the iterative Bayesian spectrum reconstruction algorithm is based on successive refinement of the spectrum estimate in individual bins. The idea proposed in the OmniFold algorithm is to extend this approach to binning-free estimates of the distribution density. The key point is to calculate the likelihood ratio estimate

$$L_{(w,X),(w',X')}(x) = \frac{p_{(w,X)}(x)}{p_{(w',X')}(x)}\,,$$

where $p_{(w,X)}(x)$ is understood as an estimate of the distribution density of a random variable obtained from a sample X with parameters (weights) w. This estimate is built using a preferred machine-learning model; in particular, the authors use the PFNs (particle flow networks) neural network algorithm [99, 100].

The main approach used in OmniFold is to consider events at the level of the detector and at the level of particles simulated by Monte Carlo methods. For training (determining the parameters), a set of pairs (t,m) is used with an event t at the particle level corresponding to an event m at the detector level, obtained (generated) by simulating the operation of the detector. The generated detector events (denoted as Sim) are transformed, with some parameters, to fit the experimental data (Data). The transformed data is used to refine the estimate of parameters and particle-level values (Gen), which are again passed to the detector level at the next step of the iterative procedure.

The considered iterative algorithm can be formally described as follows.

Initialization. Initial values of the parameters (weights) $v_0(t)$ are set at the particle level. When simulating the operation of a detector that transforms events t into m, they become parameters at the detector level: $v_0^{\text{push}}(m) = v_0(t)$.

Next, the following two steps are executed iteratively.

Step 1. Estimate the parameters at the detector level,

$$\omega_n(m) = v_{n-1}^{\text{push}}(m)\, L_{(1,\,\text{Data}),\,(v_{n-1}^{\text{push}},\,\text{Sim})}(m)\,,$$

and pass these parameters to the particle level: $\omega_n^{\text{pull}}(t) = \omega_n(m)$.

Step 2. Estimate the particle-level parameters:

$$v_n(t) = v_{n-1}(t) L_{(\omega_n^{\text{pull}},\,\text{Gen}),\,(v_{n-1},\,\text{Gen})}(t)\,.$$

After n iterations, the reconstructed quantity distribution is calculated as $p_{\text{unf}}^{(n)}(t) = v_n(t)\, p_{\text{Gen}}(t)$. The result of the algorithm can be either a set of generated events t with weights $v_n(t)$ or just the generated function $v_n(t)$, which can be applied to the measured density distribution estimated from an arbitrary data set.

Besides the main algorithm, the authors of [24] proposed versions of it that use a simpler three-layer neural network model to generate the function $L_{(w,\,X),\,(w',\,X')}(x)$. These versions can be used both for reconstructing one-dimensional distributions (the UniFold algorithm) and in the multidimensional case (the MultiFold algorithm). The authors of [24] also note that the proposed method can be used in the bin-by-bin case (to construct histogram density estimates) and can be adapted for use in other likelihood ratio generation schemes [101, 102].

3.5 Software implementations

The importance of the deconvolution problem in applied tasks, the large volumes of data to be processed, and the wide scope of application of the corresponding methods require the development of software implementations of the algorithms described in Sections 3.1–3.4.

The first widespread software product for solving such problems in elementary particle physics was the $\mathcal{RUN}$ package coded in FORTRAN 77 [1, 61], implementing the regularization algorithm for deconvolution and the smoothing of distributions with B-splines [2].

At present, the ROOT software package [49] developed at CERN is actively used to process experimental data in elementary particle physics. In ROOT, in particular, the TUnfold algorithm [37] is implemented based on the idea of regularization. In addition to the deconvolution algorithm itself, the package provides tools for binning the data and the option to combine data for analysis from various sources.

Also, the RooUnfold package [50] developed in the ROOT environment is distinguished by a variety of deconvolution algorithms implemented: the iterative Bayesian D'Agostini algorithm [38, 40], the SVD-Unfold method [36], an interface to the TUnfold algorithm implemented in ROOT, the IDS algorithm [66], and the bin-by-bin correction method. Subsequently, these methods were included in the RooFitUnfold software package [103]. Based on the ROOT libraries, the TRUEE (Time-dependent Regularized Unfolding for Economics and Engineering problems) [104] package was also developed, which is a C++ version of the $\mathcal{RUN}$ package adapted for wider use.

The bulk of the developed software is an implementation of a single algorithm or a class of methods. For example, the PyUnfold package [105] contains an implementation of the iterative Bayesian algorithm [40] modified by including a wider set of metrics to be used for stopping the iterative procedure. The algorithm based on the SVD approach [36] was originally implemented within the GURU software package [44]. In the same category of software products are the already mentioned $\mathcal{RUN}$ and TRUEE packages, in which one of the regularization methods is implemented and which had been widely used before the appearance of more efficient algorithms available in ROOT and RooUnfold. The OmniFold algorithm uses the EnergyFlow package developed by the authors of [106], which includes software tools for particle physics problems, and is also available as a Python open source [107].

Some collaborations create their own implementations of the methods, which are still based on the same approaches. For example, the PAMELA (Payload for Antimatter Matter Exploration and Light-nuclei Astrophysics) collaboration uses a PamUnfold software package that implements both (basic and modified) versions of D'Agostini's Bayesian algorithm. In some areas, highly specialized software implementations of algorithms are used, originally designed to solve specific experimental problems. For example, the already mentioned SPUNIT and BON neutron spectrum reconstruction algorithms are implemented in the BUNKI software package [108] and its modification [109], while the MAXED algorithm uses a software module of the same name. In addition, these algorithms and the SAND-II method are implemented in the BUMS package [110] featuring a web interface that allows access to the program through a browser. At the same time, the methods created for solving local problems and the software packages that implement them can also be widely used. For example, the implementation of the ${}_s\mathcal{P}lot$ algorithm [112] for processing experimental results of the BaBar collaboration [111] is included in the ROOT framework (as the TSPlot class) and is currently used to solve various problems in particle physics [113–116].

4. Use of deconvolution methods in particle physics experiments

Experiments in various fields of elementary particle physics are currently the main areas where various deconvolution methods are actively used. The most vivid example of their use and the main driver of development are accelerator experiments, where various approaches and algorithms can be encountered as an integral part of the analysis of scientific data.

Many publications describe deconvolution methods used to solve problems in experiments at the DESY (Deutsches Elektronen-Synchrotron) [117], Tevatron [118–121], SPS (Super Proton Synchrotron) [122], and LHC [1, 123] facilities. As examples, we note data analyses from the ATLAS (A Toroidal LHC ApparatuS) [124, 125] and CMS (Compact Muon Solenoid) [126, 127] detectors. There are detailed reviews devoted to the use of deconvolution methods in these experiments [41, 128].

The deconvolution methods are used in one way or another in the analysis of most of the phenomena studied at accelerators. Of particular interest in recent years is the study of processes associated with decays of the Higgs boson and

reactions involving t quarks [129, 130], since information about the true distributions of physical quantities in LHC data is important in searching for signals from the so-called New Physics — hypothetical processes that do not fit into the Standard Model framework. Because the effects of such processes are expected to be minuscule, even the most insignificant instrumental distortions must be eliminated. For example, an exotic decay of the Higgs boson with the final production of hadrons after a chain of decays is modeled in [131]. The signal from such a process could be seen as a bump on the distribution of the invariant mass of the Z-boson plus hadron jet system, and the deconvolution algorithm (specifically, OmniFold) is to be applied to it.

Neural networks based on the GAN model are used in the analysis of instrumental effects in detectors at the LHC in the study of the production of a pair of Z and W bosons and quantum chromodynamics processes [132]. The applicability of deconvolution methods to data from the ATLAS detector at the LHC was studied in detail in thesis [133].

The use of deconvolution methods is also envisaged in experiments at future accelerator complexes, for example, when processing data from the multi-purpose detector MPD that will be located at the NICA (Nuclotron-based Ion Collider fAcility) accelerator under construction in Dubna [134–136]. In this case, unfolding methods are already used at the stage of numerical simulation of the characteristics of the MPD detector to obtain the most detailed and realistic description of its characteristics [137, 138].

Another important scientific area where deconvolution methods are often used in data analysis is cosmic-ray physics. Two categories of experiments must be considered here: in space (on spacecraft and the ISS) and at ground facilities.

Operation in outer space imposes numerous restrictions on the design of the instrument (physical dimensions, power consumption, etc.), which affects both the energy resolution of the instruments and the particle detection efficiency, which can be influenced by various factors, for example, leading to an incorrect measurement of the spectrum index. In modern experiments based on magnetic spectrometry, such as BESS (Balloon-borne Experiment with Superconducting Spectrometer), PAMELA, and AMS-02 (Alpha Magnetic Spectrometer-02), deconvolution methods have been used in the analysis of the published cosmic-ray energy spectra (see, e.g., [139–146]).

For particle energies above several tens of TeV, measurements based on magnetic analysis become impossible. Instruments that determine the characteristics of particles by calorimetric methods are capable of providing measurements of cosmic-ray energies up to several PeV. In space, the main factor is the size of the calorimeter, the energy being measured by the total energy release in a cascade caused by a cosmic-ray particle. As the energy of the primary particle increases, the spatial extent of the cascade no longer fits within the calorimeter. This leads to a deteriorating resolution of the instrument and increasing error in energy measurements. As in the preceding case, a more reliable determination of the spectrum index requires the use of deconvolution methods. Examples of their use in such measurements are given in [72, 147] for the respective DAMPE (DArk Matter Particle Explorer) and CALET (CALorimetric Electron Telescope) experiments.

With a further increase in energy, particle detection in space experiments becomes impossible, and the characteristics of super- and ultrahigh-energy cosmic rays are studied by ground-based facilities whose operation is based on the registration of extensive atmospheric showers (ASs). There are two independent techniques for detecting ASs: using an array of so-called surface detectors (SDs), which register the charged component of an AS that has reached Earth's surface, and using optical systems that observe fluorescence during the development of a cascade in the atmosphere (FDs). Techniques can be combined, which increases the accuracy of the data obtained. Still, the distortion of measured characteristics can be significant due to factors such as light coming from other natural phenomena, atmospheric effects, large sizes of ultra-high-energy AS particles, and the need to place detectors at a distance from each other to cover a large area. As in calorimetric measurements, it is not possible to register ASs with the same efficiency from the point of its initiation to complete absorption.

Examples of the use of deconvolution methods in such cases can be found in publications on the results of measurements of the spectra of ultrahigh-energy cosmic rays by observatories such as the Pierre Auger Observatory (PAO) [148] or the Telescope Array [149].

Similar methods of space and ground-based measurements are used in the registration of gamma radiation in gamma astronomy. The distortions mentioned are preserved there and also require correction. The deconvolution methods used in the MAGIC experiment (Major Atmospheric Gamma Imaging Cherenkov telescopes) are described in detail in [150, 151], and those used the H.E.S.S. (High Energy Stereoscopic System) experiment, in [152]. An extensive review of such methods in gamma spectrometry can be found in [153]. Papers [154–156] describe the use of deconvolution methods in processing the energy spectra of point-like sources of gamma radiation; in [157], they are applied to the total differential energy spectrum of electrons and positrons measured by the Fermi gamma-ray space observatory.

Spectrum reconstruction methods are also widely used in neutrino physics. Due to the extremely small cross section of their interaction with matter, neutrinos are very difficult to detect. A significant amount of detector material is required for the passing high-energy neutrinos to interact with nuclei forming secondary charged particles, such as an electron or a muon. Secondary particles are registered by detectors and their characteristics are determined, which allows reconstructing information about the energy and direction of neutrino arrival. The size of the installation, the need to locate the detectors sufficiently far from each other, the quality of the target material (especially if they are natural reservoirs of ice or water), and other factors lead to a deterioration in the resolution of the installation. Therefore, taking instrumental effects into account becomes an extremely important task in reconstructing the energy spectra and spatial distributions of neutrinos of various origins.

For example, in the IceCube experiment at the South Pole, the true spectrum of atmospheric muon neutrinos is reconstructed by a procedure applied to the distributions of the number of detected muons and their energy losses [158, 159]. Similar methods are used in the ANTARES (Astronomy with a Neutrino Telescope and Abyss environmental RESearch) experiment in the Adriatic Sea and in the Baikal-GVD (Baikal Gigaton Volume Detector) experiments in Lake Baikal [160].

In addition to scientific issues, deconvolution methods are also used for practical purposes: measuring the hadron collider luminosity via elastic scattering of protons on each

other, with the true distribution over the scattering angle being reconstructed [161]; neutron spectroscopy problems [162, 163]; studies of the reactor antineutrino spectrum [164]; monitoring, detection, and identification of radioactive materials by the shape of the ionizing radiation spectrum [153]; etc.

It is important to note that the reconstruction of true distributions is required not only in the analysis of final results, such as particle spectra. With the use of deconvolution methods, the amplitudes of signals from photomultiplier tubes [19, 165–167], signal distributions in clusters of position-sensitive detectors, for example, at ALICE/LHC [168] or MPD/NICA [134–138], and other similar problems are being solved [169]. This allows obtaining more accurate information about the time of flight and velocity of particles and better reconstructing their coordinates and trajectory.

Deconvolution methods are used in the physics of not only high but also low energies, for example, in neutron spectrometry and gamma spectrometry, nuclear medicine, and biomedicine [170–172].

In the table, we list some of the best-known experiments in particle physics, space physics, and gamma-ray astronomy that use deconvolution methods to reconstruct the true characteristics of measured quantities. Examples of specific publications, a brief formulation of the physical problems being solved, and the deconvolution methods used are also indicated.

5. Prospects for the development of deconvolution methods. Conclusions

The deconvolution methods to reconstruct the true distributions of physical quantities are now widely used in various scientific fields, are actively discussed at scientific conferences and dedicated schools (Terascale Statistics School, Pan-European Advanced School on Statistics in High Energy Physics, etc.), and are part of training courses on statistical methods and their applications [8, 187–189]. However, there is no general universal approach that has been successfully used in different experiments, and additional research is required in each case. In this regard, it is important to develop all possible approaches and propose new methods for solving the deconvolution problem.

At the same time, a detailed comparative analysis of various methods is needed in order to see their limitations and specificity of use, for example, to reveal the dependence

Table. Examples of the use of deconvolution methods to reconstruct true distributions of measured physical quantities.

Experiment	Physical problem	References	Method
Accelerator experiments			
ATLAS/LHC	Measurement of the four-lepton decay cross section of the Higgs boson	[71]	Bin-by-bin correction method
CMS/LHC	Measurement of charge asymmetry in top-quark pair production in proton–proton collisions	[126]	TUnfold
ALFA/LHC	Measurement of the elastic scattering cross section in proton collisions for measuring the LHC luminosity	[161]	Iterative methods
Tevatron/Fermilab	Study of the production and decay properties of a top quark–antiquark pair	[118]	Regularization
HERA/DESY	Study of correlations in lepton and hadron jet production in deep inelastic proton scatterings	[117]	OmniFold
KLOE/DAΦNE*	Measurement of the pion form factor in electron–positron collisions to study the anomalous magnetic moment of the muon	[173]	Bayesian
BEPC/BES III**	Study of Ψ-meson production and decay processes	[174]	Other methods
CBM/FAIR***	Study of possible deviations from the charge conservation law in gold–gold collisions	[175]	Bayesian
Cosmic rays			
AMS-02	Magnetospectrometric measurements of the energy spectra of galactic cosmic ray (GCR) protons	[176]	Bayesian
FERMI	Calorimetric measurements of the energy spectrum of GCR protons	[177]	TUnfold
PAMELA	Magnetospectrometric measurements of the spectra of antiprotons, positrons, and nuclei	[140, 141, 178]	Bayesian
DAMPE	Calorimetric measurements of the spectra of GCR protons and helium nuclei	[147, 179]	Bayesian
CALET	Calorimetric measurements of the spectra of the GCR nuclear component	[72, 180]	RooUnfold
PAO	Measurement of the spectrum of cosmic rays with energies above 2.5×10^{18} eV	[181]	Bin-by-bin correction method
Gamma astronomy			
MAGIC	Measurement of the gamma-radiation spectrum from pulsars	[182, 183]	Regularization, 'naive' approach
H.E.S.S.	Measurement of gamma-radiation spectra from astrophysical sources in the Crab Nebula and PKS 2155-304	[152]	Bayesian

Table (continued)

Experiment	Physical problem	References	Method
Neutrino studies			
IceCube	Measurement of astrophysical neutrino fluxes from point sources	[184, 185]	*RUN* (TRUEE)
ANTARES, Baikal-GVD	Measurement of energy spectra of atmospheric neutrinos	[160]	—
Super Kamiokande	Measurement of atmospheric neutrino and antineutrino fluxes	[186]	RooUnfold package
Daya Bay	Measurement of reactor antineutrino spectra	[164]	Wiener-SVD

* K LOng Experiment/Double Annular Φ Factory for Nice Experiments.
** Beijing Electron – Positron Collider/Beijing Spectrometer III.
*** Compressed Baryonic Matter/Facility for Antiproton and Ion Research.

of the result on the range of values of a physical quantity, binning methods, the spectral features of a physical quantity, and other parameters. It is also necessary to propose a strategy for the optimal selection of the parameters of the methods themselves and for estimating the error in reconstructing the true distribution by different algorithms [190], which will allow drawing conclusions regarding the best suitability of the methods in various scientific problems.

Based on such an analysis, it is possible to develop new algorithms for solving the problem, including those relying on mathematical approaches that have not yet been used in deconvolution methods. Such studies are appearing in print (see, e.g., [24, 32, 42, 64, 191–193]).

Other important tasks include the design of new and development of existing reconstruction methods for multidimensional distributions [67, 194, 195]. For algorithms based on the Bayesian approach (the iterative D'Agostini algorithm and the IDS and FBU methods), it is critical to reduce the average number of events in a bin (for a fixed average size, the number of bins increases sharply with increasing spatial dimension). We also note that Tikhonov's regularization used in the one-dimensional case requires assigning adjacent bins the adjacent numbers (those differing by unity). In the multidimensional case, in general, there is no numbering of multidimensional bins that assigns close numbers to spatially close bins. For this reason, directly carrying over regularization methods to the multidimensional case is difficult and requires their adaptation. Nevertheless, the previously described applied problems of analyzing the effectiveness of various spectrum reconstruction algorithms by no means lose their relevance and complexity in the multidimensional case.

This paper was supported by a grant from the Russian Science Foundation (project 19-72-10161).

References

1. Blobel V, in *Proc. of the 1984 CERN School of Computing, Aiguablava, Catalonia, Spain, 9–22 September 1984* (CERN 85–09) (Geneva: CERN, 1985) pp. 84–114
2. Blobel V, hep-ex/0208022
3. Rust B W, Ingersoll D T, Burrus W R *A User's Manual for the FERDO and FERD Unfolding Codes* (Oak Ridge, TN: Oak Ridge National Laboratory, 1983)
4. Engl H W, Hanke M, Neubauer A *Regularization of Inverse Problems* (Dordrecht: Kluwer Acad. Publ., 2000)
5. Cowan G, in *Proc. Conf. on Advanced Statistical Techniques in Particle Physics* (Eds M R Whalley, L Lyons), IPPP/02/39, Durham 2002
6. Kaipio J, Somersalo E *Statistical and Computational Inverse Problems* (New York: Springer, 2005)
7. Barlow R, in *Proc. PHYSTAT2003, SLAC, Stanford, California, September 8–11, 2003*
8. Cowan G *Statistical Data Analysis* (Oxford: Clarendon Press, 1998)
9. Blobel V, in *PHYSTAT2011 Workshop on Statistical Issues Related to Discovery Claims in Search Experiments and Unfolding*
10. Behnke O et al. *Data Analysis in High Energy Physics*: *A Practical Guide to Statistical Methods* (Weinheim: Wiley-VCH, 2013)
11. Span'o F *EPJ Web Conf.* 55 (2013)
12. Schmitt S, arXiv:1611.01927; *EPJ Web Conf.* **137** 11008 (2017)
13. Hansen P C *Discrete Inverse Problems — Insight and Algorithms* (Ohio, OH: SIAM, 2010)
14. Zech G, arXiv:1607.06910
15. Egorov A Yu et al. *St. Petersburg Polytech. State Univ. J. Phys. Math.* **12** (3) (2019)
16. Adye T, arXiv:1105.1160; in *Proc. of the PHYSTAT 2011 Workshop, CERN, Geneva, Switzerland, January 2011*, CERN-2011-006
17. Brenner L et al., arXiv:1910.14654
18. Klepser S "Reconstruction of Extensive Air Showers and Measurement of the Cosmic Ray Energy Spectrum in the Range of 1–80 PeV at the South Pole", Dissertation Dr. rer. nat. (Berlin: Mathematisch-Naturwissenschaftlichen Fakultat I Humboldt-Univ. zu Berlin, 2008)
19. Niederhausen H "Measurement of the High Energy Astrophysical Neutrino Flux Using Electron and Tau Neutrinos Observed in Four Years of IceCube Data", PhD Thesis (New York: Stony Brook Univ., 2018)
20. Hartmann S "On the unfolding of the energy spectrum measured by the HEAT extension at the Pierre Auger Observatory", Master Deg. Dissertation (Aachen: RWTH Aachen Univ., 2015)
21. Geenen H "Reconstruction of the Primary Energy Spectrum from Fluorescence Telescope Data of the Pierre Auger Observatory", Dissertation (Wuppertal: Univ. of Wuppertal, 2007)
22. Zech G, Aslan B, in *Proc. PHYSTAT 2003, Stanford, USA, September 8–11, 2003*
23. Dembinski H P, Roth M *Nucl. Instrum. Meth. Phys. Res. A* **729** 410 (2013)
24. Andreassen A et al. *Phys. Rev. Lett.* **124** 182001 (2020); arXiv:1911.09107
25. Arratia M et al. *JINST* **17** P01024 (2022); arXiv:2109.13243
26. Rosenblatt M *Ann. Math. Statist.* **27** 832 (1956)
27. Chentsov N N *Dokl. Akad. Nauk SSSR* **147** 45 (1962)
28. Gu C, Qui C *Ann. Statist.* **21** (1) 217 (1993)
29. Loftsgaarden D O et al. *Ann. Math. Stat.* **36** 1049 (1965)
30. Aizerman M A, Braverman E M, Rozonoer L I *Metod Potentsial'nykh Funktsii v Teorii Obucheniya Mashin* (Method of Potential Functions in Machine Learning Theory) (Moscow: Nauka, 1970)
31. Kuusela M "Statistical Issues in Unfolding Methods for High Energy Physics", Master Thesis (Espoo: Aalto Univ., 2012)
32. Vischia P, arXiv:2009.02913
33. MicroBooNE Collab. "MicroBooNE low-energy excess signal prediction from unfolding MiniBooNE Monte-Carlo and data", MICROBOONE-NOTE-1043-PUB MicroBooNE docdb-15587, 2018
34. Bohm G, Zech G *Introduction to Statistics and Data Analysis for Physicists* (Hamburg: Verlag Deutsches Elektronen-Synchrotron, 2017)
35. Kuusela M, Stark P B, arXiv:1512.00905

36. Höcker A, Kartvelishvili V *Nucl. Instrum. Meth. Phys. Res. A* **372** 469 (1996)
37. Schmitt S *JINST* **7** (10) T10003 (2012)
38. D'Agostini G *Nucl. Instrum. Meth. Phys. Res. A* **362** 487 (1995)
39. Bierwagen K, in *Proc. Workshop on Statistical Issues Related to Discovery Claims in Search Experiments and Unfolding, PHYSTAT 2011, CERN, Geneva, Switzerland, 17–20 January 2011* (Eds H B Prosper, L Lyons) CERN–2011–006
40. D'Agostini G, arXiv:1010.0632
41. Kuusela M, Panaretos V M *Ann. Appl. Stat.* **9** 1671 (2015)
42. Baroň P *Acta Phys. Polon. B* **51** 1241 (2020)
43. Choudalakis G, arXiv:1201.4612
44. Kartvelishvili V, in *Proc. Workshop on Statistical Issues Related to Discovery Claims in Search Experiments and Unfolding* (*PHYSTAT 2011*), *CERN, Geneva, Switzerland, 17–20 January 2011* (Eds H B Prosper, L Lyons); CERN–2011–006
45. Richardson W H *J. Opt. Soc. Am.* **62** (1) 55 (1972)
46. Lucy L B *Astron. J.* **79** 745 (1974)
47. Zech G *Nucl. Instrum. Meth. Phys. Res. A* **716** 1 (2013)
48. Licciardi M, Quilain B, arXiv:2101.01096
49. Official website of ROOT package, https://root.cern.ch/
50. Official website of RooUnfold package, http://hepunx.rl.ac.uk/~adye/software/unfold/RooUnfold.html
51. Lavička R "Ultra-Peripheral Collisions at ALICE", Dissertation Thesis (Prague: Czech Technical Univ. in Prague, 2021); CERN-THESIS-2021-111
52. Tikhonov A N *Sov. Math. Dokl.* **4** 1035 (1963); *Dokl. Akad. Nauk SSSR* **151** 501 (1963)
53. Adye T, in *Proc. Workshop on Statistical Issues Related to Discovery Claims in Search Experiments and Unfolding, PHYSTAT 2011, CERN, Geneva, Switzerland, 17–20 January 2011* (Eds H B Prosper, L Lyons) p. 313; CERN–2011–006
54. Schmelling M *Nucl. Instrum. Meth. Phys. Res. A* **340** 400 (1994)
55. Narayan R, Nityananda R *Annu. Rev. Astron. Astrophys.* **24** 127 (1986)
56. Dembinski H P, Roth M, in *Proc. Workshop on Statistical Issues Related to Discovery Claims in Search Experiments and Unfolding* (*PHYSTAT 2011*), *CERN, Geneva, Switzerland, 17–20 January 2011* (Eds H B Prosper, L Lyons) p. 285; CERN–2011–006
57. Green P J, Silverman B W *Nonparametric Regression and Generalized Linear Models* (London: Chapman and Hall, 1994)
58. Lee T C M *Comput. Statistics Data Analysis* **42** 139 (2003)
59. Volobouev I, arXiv:1408.6500
60. Veklerov E, Llacer J *IEEE Trans. Med. Imaging*. **6** (4) 313 (1987)
61. Blobel V, OPAL Technical Note TN361 (1996)
62. Press W H et al. *Numerical Recipes in FORTRAN*: *The Art of Scientific Computing* 2nd ed. (Cambridge: Cambridge Univ. Press, 1992)
63. Takiya C et al. *Nucl. Instrum. Meth. Phys. Res. A* **523** 186 (2004)
64. Tang W et al. *JINST* **12** P10002 (2017)
65. Malaescu B, arXiv:0907.3791; LAL 09-107
66. Malaescu B, arXiv:1106.3107; CERN-PH-EP-2011-111
67. Malaescu B, in Lectures for PhD students, Geneva, 2018
68. Lyons L, in *Proc. Workshop on Statistical Issues Related to Discovery Claims in Search Experiments and Unfolding* (*PHYSTAT 2011*), *CERN, Geneva, Switzerland, 17–20 January 2011* (Eds H B Prosper, L Lyons) p. 225; CERN-2011-006.225
69. Anykeyev V, Spiridonov A, Zhigunov V *Nucl. Instrum. Meth. Phys. Res. A* **322** (1992)
70. "Statistical Methods in Particle Physics", Heidelberg Univ., WS 2020/21, https://www.physi.uni-heidelberg.de/~reygers/lectures/2020/smipp/
71. Stahlman J M, Ph.D. Thesis (2014) at Publicly Accessible Penn Dissertations 1455
72. Adriani O et al. (CALET Collab.) *Phys. Rev. Lett.* **125** 251102 (2020); arXiv:2012.10319
73. van Cittert P H *Z. Phys.* **69** 298 (1931)
74. Burger H C, van Cittert P H *Z. Phys.* **79** 722 (1932)
75. Gold R, Report ANL-6984 (Lemont, IL: Argonne National Laboratory, 1964)
76. Ter-Antonyan S V *Astropart. Phys.* **28** 321 (2007); arXiv:0706.4087
77. Morháč M *Nucl. Instrum. Meth. Phys. Res. A* **559** 119 (2006)
78. Eichstädt S et al. *Metrologia* **50** 107 (2013)
79. Simon A et al. *J. High Energy Phys.* **2021** 146 (2021)
80. Li M et al. *Res. Astron. Astrophys.* **19** 145 (2019)
81. Doroshenko J J et al. *Nucl. Technol.* **33** 296 (1977)
82. Sanna R S, Technical Report EML-394, Environmental Measurements Laboratory, August 1981
83. McElroy W W et al., Technical Report AFWL-TR-67-41, US Air Force Weapons Laboratory, 1967
84. Routti J T, Sandberg J V *Radiat. Prot. Dosim.* **10** (1–4) 103 (1985)
85. Reginatto M, Goldhagen P, Technical Report EML-595, Environmental Measurements Laboratory, June 1998
86. Chen Y H et al. *Sci. China Phys. Mech. Astron.* **57** 1885 (2014)
87. Boszon A S "Measurements of Hadronic $t\bar{t}$ Differential Cross Sections with ATLAS and Unfolding with Gaussian Processes", PhD Thesis (London: Univ. of London, 2020)
88. Koch L *JINST* **14** P09013 (2019); arXiv:1903.06568
89. Held A, Analysis Syst. Typical Workshop Report, New York, June 19–20, 2019; https://indico.cern.ch/event/822074/contributions/3471458/
90. D'Agostini G, slides for report at Alliance Workshop on Unfolding and Data Correction, Hamburg, Germany, 27–28 May 2010; https://www.roma1.infn.it/ dagos/unf2_hh.pdf
91. Datta K, Kar D, Roy D, arXiv:1806.00433
92. Gagunashvili N D, arXiv:1004.2006
93. Glazov A, arXiv:1712.01814; DESY-17-214
94. Isildak B, arXiv:2001.10814
95. Goodfellow I J et al., arXiv:1406.2661
96. Butter A, Plehn T, arXiv:2008.08558
97. ARU project website, https://aru.hepforge.org/
98. de Boor C *A Practical Guide to Splines* (New York: Springer-Verlag, 1978)
99. Komiske P T, Metodiev E M, Thaler J *J. High Energy Phys.* **2019** (01) 121 (2019); arXiv:1810.05165
100. Zaheer M et al., in *Advances in Neural Inf. Proc. Systems 30*: *Annual Conf. on Neural Information Processing Systems 2017, 4–9 December 2017, Long Beach, CA, USA* (2017)
101. Cranmer K, Pavez J, Louppe G, arXiv:1506.02169
102. Bothmann E, Del Debbio L *J. High Energy Phys.* **2019** 33 (2019)
103. Brenner L et al. *Int. J. Mod. Phys. A* **35** 2050145 (2020)
104. Milke N et al. *Nucl. Instrum. Meth. Phys. Res.* **697** 133 (2013)
105. Bourbeau J, Hampel-Arias Z *J. Open Source Software* **3** (26) 741 (2018)
106. Komiske P T, Metodiev E M, EnergyFlow package, 2019, https://energyflow.network/
107. Komiske P T, Metodiev E M, OmniFold package, 2021, https://github.com/pkomiske/OmniFold
108. Lowry K A, Johnson T L *Health Phys.* **47** 587 (1984)
109. De Sousa Lacerda M A et al., in *Proc. of the 18th Intern. Symp. on Solid State Dosimetry, Oaxaca, Mexico, 24–28 Sep. 2018*
110. Sweezy J, Hertel N, Veinot K *Nucl. Instrum. Meth. Phys. Res. A* **476** 263 (2002)
111. Pivk M, BABAR-THESIS-03/012 (2003)
112. Pivk M, Le Diberder F R *Nucl. Instrum. Meth. Phys. Res. A* **555** 356 (2005)
113. Aaij R et al. *J. High Energy Phys.* **2022** (01) 065 (2022)
114. Anderlini L, arXiv:2110.07925
115. Mathad A et al. *JINST* **16** (06) P06016 (2021)
116. Artamonov A V "Issledovanie rozhdeniya $\Upsilon(nS)$ mezonov v pp-vzaimodeistviyakh pri $\sqrt{s} = 7$ и 8 TeV v eksperimente LHCb" ("Investigation of the production of $\Upsilon(nS)$ mesons in pp interactions at $\sqrt{s} = 7$ and 8 TeV in the LHCb experiments"), Thesis for Candidate of Phys.-Math. Sciences (Protvino: Logunov Institute for High Energy Physics, National Research Center Kurchatov Institute, 2019)
117. Andreev V et al. (H1 Collab.), arXiv:2108.12376; DESY 21-130
118. Wagner W *Mod. Phys. Lett. A* **25** 1297 (2010)
119. Gresham M I, Kim I-W, Zurek K M *Phys. Rev. D* **83**114027 (2011)
120. Abazov V M et al. (D0 Collab.) *Phys. Rev. Lett.* **101** 191801 (2008)
121. Aaltonen T et al. (CDF Collab., D0 Collab.) *Phys. Rev. D* **97** 112007 (2018)
122. Prokhorova D S, Andronov E V *J. Phys. Conf. Ser.* **1690** 012134 (2020)
123. Evans L R, Bryant P *JINST* **3** S08001 (2008)
124. Kohn F, Ph.D. Thesis (Göttingen, 2012)

125. ATLAS Collab. *Eur. Phys. J. C* **72** 2039 (2012)
126. Chatrchyan S et al. (CMS Collab.) *Phys. Lett. B* **709** 28 (2012)
127. Savitskyi M "Measurements of differential cross sections for $t\bar{t}$ production in proton-proton collisions at $\sqrt{s} = 13$ TeV using events containing two leptons with the CMS experiment", Dissertation (Hamburg: Univ. of Hamburg, 2018)
128. Biondi S *Eur. Phys. J. Conf.* **137** 11002 (2017)
129. Sirunyan A M et al. (CMS Collab.) *J. High Energy Phys.* **2021** (03) 257 (2021)
130. Wagner-Kuhr J, arXiv:1606.02936
131. Komiske P, McCormack W P, Nachman W *Phys. Rev. D* **104** 076027 (2021); arXiv:2105.09923
132. Bellagente A et al. *SciPost Phys.* **9** 074 (2020)
133. Herrmann T "Study of Different Unfolding Methods of Kinematic Distributions of the WZ→WZ Scattering with Data and Simulation of the ATLAS Detector at the LHC", Dissertation (Dresden: Technical Univ. of Dresden, 2017)
134. Agapov N N et al. *Phys. Usp.* **59** 383 (2016); *Usp. Fiz. Nauk* **186** 405 (2016)
135. Kolesnikov V et al. *Phys. Part. Nucl. Lett.* **16** 6 (2019)
136. Butenko A V et al. *Phys. Usp.* **66** 195 (2023); *Usp. Fiz. Nauk* **193** 206 (2023)
137. Drnoyan J et al., report at The Conference "RFBR Grants for NICA", Evaluation of prospects for hypernuclei studies with MPD at NICA — JINR, Dubna, Russia, 20–23 October 2020
138. Geraksiev N, report at Workshop on analysis techniques for centrality determination and flow measurements at FAIR and NICA (FANI-2020) Anisotropic flow of Λ-hyperons in MPD@NICA. — NRNU "MEPhI", Moscow, 24–28 August 2020; http://indico.oris.mephi.ru/event/181/session/1/contribution/16/
139. Abe K et al. *Astrophys. J.* **822** 65 (2016)
140. Adriani O et al. *Phys. Rev. Lett.* **111** 081112 (2013)
141. Adriani O et al. *Phys. Rev. Lett.* **105** 121101 (2010)
142. Adriani O et al. *Astrophys. J.* **810** 142 (2015); arXiv:1512.01079
143. Adriani O et al. *Science* **332** 69 (2011)
144. Casaus J *J. Phys. Conf. Ser.* **631** 012046(2015)
145. Ghelfi A, in *Cosmic Rays & their Interstellar Medium Environment* (*CRISM-2014*), *June 2014, Montpellier, France, Proc. of Science, CRISM2014*, p. 013
146. Aguilar M et al. *Phys. Rev. Lett.* **126** 041104 (2021)
147. Wang Z "Measurement of Cosmic Ray Proton + Helium Flux with the DAMPE Experiment", Dissertation (Gran Sasso Science Institute, 2020)
148. Verzi V, Ivanov D, Tsunesada Y *Prog. Theor. Exp. Phys.* **2017** (12) 12A103 (2017)
149. Ivanov D "Energy spectrum measured by the telescope array surface detector", Thesis for Doctor of Philosophy Graduate Program in Physics and Astronomy (New Brunswick, NJ: Rutgers, The State Univ. of New Jersey, 2012) https://doi.org/10.7282/T3K35SG3
150. Curtef V "A new unfolding method for the MAGIC telescope", Thesis for the Doctor of Physics (Dortmund: Univ. of Dortmund, 2008) https://doi.org/10.17877/DE290R-874
151. Albert J et al. *Nucl. Instrum. Meth. Phys. Res. A* **583** 494 (2007); arXiv:0707.2453
152. Oberndörfer M "Bayesian Unfolding of H.E.S.S. energy spectra", Masterarbeit aus der Physik (Erlangen-Nürnberg: Erlangen Centre for Astroparticle Physics, Friedrich-Alexander-Univ., 2017)
153. Fei Li et al. *Results Phys.* **13** 102211 (2019)
154. Loparco F, Mazziotta M N, arXiv:0912.3695
155. Mazziotta M N, arXiv: 0912.1236
156. Abdo A A et al. *Astrophys. J. Suppl. Ser.* **187** (2) (2010)
157. Mazziotta M N, arXiv:0907.0638
158. Sandroos J, arXiv:1909.07174; PoS-ICRC2019-999
159. Abbasi R *Phys. Rev. D* **83** 012001 (2011)
160. Schüssler F on behalf of the ANTARES Collab. *EPJ Web Conf.* **121** 05002 (2016)
161. Trzebinski M, Staszewski R, Chwastowski J *ISRN High Energy Physics* **2012** 491460 (2012)
162. Wang Z et al. *Nucl. Technol.* **168** 610 (2009)
163. Reginatto M, Goldhagen P, Neumann S *Nucl. Instrum. Meth. Phys. Res. A* **476** 242 (2002)
164. An F P et al. (Daya Bay Collab.) *Chinese Phys. C* **45** (7) 073001 (2021); arXiv:2102.04614
165. Zhu N M *IEEE T Nucl. Sci.* **66** 2265 (2019)
166. Peterson J H *J. Instrum.* **16** C09032 (2021)
167. Aartsen M G *J. Instrum.* **9** P03009 (2014)
168. Zinchenko A, Chabratova G *Nucl. Instrum. Meth. Phys. Res. A* **502** (2–3) 778 (2003)
169. Blobel V, Kleinwort C, hep-ex/0208021; DESY 02-077
170. Reginatto M *Radiat. Meas.* **45** 1323 (2010)
171. Dommert M *Current Directions Biomed. Eng.* **3** (2) 83 (2017)
172. Zimbal A, at ECPD 2015 – 1st EPS Conf. on Plasma Diagnostics – Frascati – Proc. of Science (ECPD2015)
173. Venanzoni G *AIP Conf. Proc.* **1182** 665 (2009)
174. Ablikim M *Chinese Phys. C* **37** 063001 (2013)
175. Samanta S *Nucl. Phys. A* **1005** 121896 (2021); arXiv 2002.12235
176. Aguilar M et al. (AMS Collab.) *Phys. Rev. Lett.* **114** 171103 (2015)
177. Green D M, PhD Thesis (College Park, MD: Univ. of Maryland, 2016)
178. Adriani O et al. *Astrophys. J.* **791** 93 (2014)
179. An Q et al. *Sci. Adv.* **5** eaax3793 (2019)
180. Adriani O et al. *Phys. Rev. Lett.* **126** 241101 (2021)
181. Aab A et al. *Phys. Rev. D* **102** 062005 (2020)
182. Zanin R "Observation of the Crab pulsar wind nebula and microquazar candidates with MAGIC", Ph.D. Dissertation (Bellaterra (Barcelona), Spain: Univ. Autonoma de Barcelona, 2011)
183. Albert J et al. *Astrophys. J.* **663** 125 (2007)
184. Aartsen M G et al. (IceCube Collab.) *Eur. Phys. J. C* **77** (10) 692 (2017)
185. Aguilar J A et al. (IceCube Collab.) *Eur. Phys. J. Part. Fields* **75** (3) 116 (2015)
186. Richard E et al. *Phys. Rev. D* **94** 052001 (2016)
187. "Statistical methods 2021", Institute of Particle and Nuclear Physics, https://ipnp.cz/?page_id = 4280
188. Logashenko I B *Metody Analiza Eksperimental'nykh Dannykh. Elektronnyi Lektsionnyi Kurs* (Methods of Analysis of Experimental Data. Electronic Lecture Course) (Novosibirsk: NGU, 2013)
189. Logashenko I B, Eidel'man S I *Phys. Usp.* **61** 480 (2018); *Usp. Fiz. Nauk* **188** 540 (2018)
190. Alekseev V V et al. *J. Phys. Conf. Ser.* **1390** 012071 (2019)
191. Baron P, arXiv:2001.05877
192. Wei X et al. *IEEE Trans. Signal Process.* **70** 2962 (2022); arXiv:2107.02848
193. Pop F *Adv. High Energy Phys.* **2014** 507690 (2014)
194. Kuusela M, in PhyStat-ν 2019, CERN, Geneva, Switzerland
195. Kuusela M, CP3 Remote Seminar Report (Univ. Catholique de Louvain), July 1, 2020, https://agenda.irmp.ucl.ac.be/event/4000/